CAPNOGRAPHY AND THE BAIN CIRCUIT II: VALIDATION OF A COMPUTER MODEL

Jan E. W. Beneken, PhD,†*
*Nikolaus Gravenstein, MD,**
*Samsun Lampotang, ME,**
*Jan J. van der Aa, Ir,**
*and Joachim S. Gravenstein, MD**

Beneken JEW, Gravenstein N, Lampotang S, van der Aa JJ, Gravenstein JS. Capnography and the Bain Circuit II: validation of a computer model.
J Clin Monit 1987;3:165–177

ABSTRACT. Validation of a computer model is described. The behavior of this model is compared both with mechanical ventilation of a test lung in a laboratory setup that uses a washout method and with manual ventilation. A comparison is also made with results obtained from a volunteer breathing spontaneously through a Bain circuit and with results published in the literature. This computer model is a multisegment representation of the Bain circuit and connecting tubing. For each segment, gas pressure, gas volume flow, and partial pressure of carbon dioxide are calculated for any number of breaths wanted. As a result, the time course of these variables can be generated for any location or, conversely, the carbon dioxide distribution in the system can be calculated for any time instant. A test lung, the human lungs, the ventilator bellows, and the reservoir bag are each represented by a single segment. The shapes of pressure and flow curves and of the capnograms taken at different locations in the Bain tubing are in good agreement. The washout study permits measurement of the time delay between the first expiration and the arrival of carbon dioxide at a particular location. The carbon dioxide level in the test lung decreases during inspiration and is stable during expiration. Quantitative agreement between model and experimental transport delays and carbon dioxide levels is such that the differences can be explained by the inaccuracy of the measurement. This is concluded from a sensitivity analysis. The study of the effect of segment size shows an almost optimal agreement between model behavior and experimental results for a 36-segment model. Execution of a thorough validation is imperative before such models can be used for clinical management and decision making or for teaching.

KEY WORDS. Monitoring: noninvasive; carbon dioxide; capnography; respiratory pressure; respiratory flow. Equipment: Bain circuit; computer simulation; computer model.

A previous article presented an extensive analysis of capnography during use of the Bain circuit, by means of a computer simulation. The physical and mathematical basis of this model was given, along with some preliminary results [1]. Such a model can be used for improved understanding of unexpected clinical situations, for teaching, and for planning and developing ventilation strategies for patients. Because far-reaching conclusions can be drawn from model behavior, it is important to validate such a model, demonstrating a quantitative agreement between the model and the reality it tries to mimic.

Initial experiments with the Bain circuit model showed peculiar time courses of the partial pressure of carbon dioxide (P_{CO_2}) in different locations of the circuit and connecting tubing. One approach to validation is, therefore, to confirm these peculiar time courses under laboratory conditions. To that end, we devised a carbon

From the *Department of Anesthesiology, University of Florida College of Medicine, Gainesville, FL 32610-0254, and †Division of Medical Electrical Engineering, Eindhoven University of Technology, Eindhoven, The Netherlands.

Received Aug 27, 1986, and in revised form Feb 2, 1987. Accepted for publication Feb 12, 1987.

Address correspondence to Dr Beneken, Division of Medical Electrical Engineering, Eindhoven University of Technology, PO Box 513, 5600 MB Eindhoven, The Netherlands.

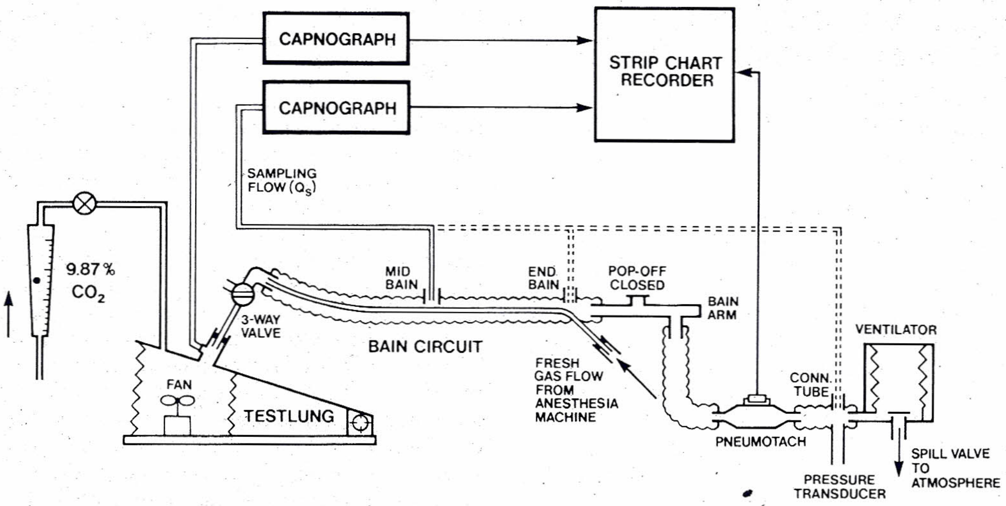

Fig 1. Experimental setup for washout studies. The dashed line representing the sampling tube indicates the connection to the two other sampling sites. Sampling occurred at only one port at a time; ports were properly sealed when not in use. CONN. TUBE = *connecting tube.*

dioxide (CO_2) washout experiment and compared, both qualitatively and quantitatively, the results from the physical experiment with those from the model. In our second and third experiments, we tested the validity of the model during manual ventilation of a test lung and against data collected during spontaneous ventilation using the Bain system. Gas pressures and flow rates were measured, and capnograms were obtained near the mouthpiece.

This article reports on these experiments and discusses the validity of the model and its usefulness.

METHODS

Experimental Setup

An experiment (Fig 1) was devised with a setup similar to that used by Gravenstein et al [2]. A small fan was installed inside the test lung (Vent Aid, Michigan Instruments Inc, Grand Rapids, MI) to ensure permanent and complete mixing of gases. A gas mixture containing 9.87% CO_2 was introduced into the test lung and subsequently out into the room through a three-way valve. The Bain circuit (Respiratory Care, Inc, Arlington Heights, IL) was connected with the ventilator (Ohio 7000 Electronic, Ohio Medical Products, Madison, WI) by a conventional Bain arm, a connecting ventilator tube, a Fleisch pneumotachograph (Dynasciences, Blue Bell, PA), and a sampling port for pressure and partial pressure measurements. Sampling ports were also located at the distal end of the Bain circuit and at a position equidistant from both ends of the Bain circuit. Capnograms at these three positions were obtained by means of a Godart 17070 infrared capnograph (Scott Instruments, Inc, Miami, FL). This capnograph has a rise time (10 to 90%) of 0.3 second. An IL 200 capnograph (Instrumentation Laboratory, Inc, Lexington, MA) took continuous samples from the test lung. The rise time of this instrument was 0.6 second.

Both capnographs drew sampling flows of 200 ml/min; their synchronization at the 10% level was obtained by adjusting the length of the sample tubing. A typical delay was 0.45 second. Because the appearance times were determined on the basis of the initial deflections, the differences between the rise times of the two capnographs had a negligible effect on the accuracy. In addition, all signal changes are of low frequency and can be followed adequately by the capnographs.

The system was accepted as free of leaks if at a pressure of 8 mm Hg and with the capnographs disconnected the decrease in pressure was less than 1 mm Hg during two and one half minutes. Once the test lung P_{CO_2} reached a stable value, the CO_2 flow was stopped, the three-way valve was turned to connect the lung with the Bain circuit, and the ventilator was turned on, starting with an inspiration. Ventilation and CO_2 washout from the test lung continued until the P_{CO_2} values had almost reached zero.

During each run the following signals were measured and recorded on the strip-chart recorder: the driving pressure just outside the ventilator, the gas flow rate in the connecting tube, two capnograms, and a 1-second timing signal. Runs were repeated to obtain capnograms at the three sampling sites. The ventilator setting was as follows: minute ventilation, 4.5 L/min; fresh-gas flow, 5.3 and 10.3 L/min; respiratory rate, 8 breaths/

Table 1. Physical Constants of the Experimental Setup for the Washout Tests

Constant	Value
Volume of test lung in collapsed position	560 ml
Compliance of test lung	140 ml/mm Hg
Volume of tubing between test lung and three-way valve (endotracheal tube)	93 ml
Volume of three-way valve and elbow connector	48 ml
Volume of Bain tubing	510 ml
Volume of Bain arm	28 ml
Volume of connecting tube between Bain arm and ventilator, inclusive pneumotachograph	558 ml
Volume of filled ventilator bellows	2,300 ml
Resistance of endotracheal tubing	0.00125 mm Hg/ml/s
Resistance of Bain and connecting tubing	0.0050 mm Hg/ml/s
Pop-off pressure of spill valve	0.60 mm Hg
Resistance of ventilator spill valve	0.0040 mm Hg/ml/s
Resistance of ventilator expiratory flow control valve	0.0040 mm Hg/ml/s

min; and expiratory-to-inspiratory ratio, 2.0. The ventilator design allowed a continuous fresh-gas flow of 300 ml/min to bypass the rotameters, the setting of which was easier and more reproducible at 5 L/min and 10 L/min; thus, the fresh-gas flow values used came out as 5.3 L/min and 10.3 L/min.

Simultaneous measurements of the capnogram in the test lung and at one of the three sites in the tubing were essential for the appearance time measurements; the test lung curve (also called the "alveolar curve") served as a reference. The prior synchronization of capnograph traces allowed accurate measurements of the appearance time of CO_2 at each of the tube sampling sites relative to the initial downward deflection of the alveolar capnogram during the first inspiration of each run. To avoid uncertainty, appearance time was defined as the time when a CO_2 level of 1.0 mm Hg was reached. Table 1 gives the physical properties of the experimental setup. Volumes of tubing and connectors were determined by filling the parts with water and measuring the respective contents in a graduated cylinder. Resistances to flow were obtained by passing known gas flow rates through the tubing and measuring corresponding decreases in pressure across the tubing. The physical constants are used as parameters in the simulation of the Bain model.

In the second experiment, which compared experimental and model results under a different set of conditions, the test lung was ventilated by means of a reservoir bag connected with the Bain arm and compressed by an experienced anesthesiologist. An inflow of 100% CO_2 to the test lung at a constant rate of 200 ml/min represented the physiological delivery of CO_2 to the lung. This experiment was performed with a fresh-gas flow rate of 4 L/min. The sampling flow was set at 200 ml/min. Other physical quantities are listed in Table 1. Gas flow rate and pressure were measured at the bag connection, and a capnogram was obtained from a sampling site between the elbow junction at the proximal end of the Bain tubing and the "endotracheal tube" of the test lung. This site was chosen on the basis of results described by Gravenstein et al [2] from their study of fresh-gas mixing and sampling sites when using the Bain circuit.

In the third experiment, measurements were made while a volunteer breathed spontaneously through a mouthpiece into the Bain circuit. The circut was connected to the Bain arm with an open pressure relief valve and a 2-liter bag. The fresh-gas flow rate was 4 L/min. Resistance of airway and mouthpiece was estimated to be 0.001 mm Hg/ml/min; the combined lung-thorax compliance of the volunteer was 160 ml/mm Hg, and his functional residual capacity was 4,200 ml. The sampling flow rate of the capnograph was 200 ml/min. For these experiments, pressure and flow were measured between the Bain circuit and the Bain arm, whereas the capnogram was obtained from the same sampling site as during manual ventilation.

Model Considerations

A full description of the Bain model is given by Beneken et al [1]. The basic concept involves transport of CO_2 in the breathing tubes by moving gas back and forth. On the basis of flow rates and the respective volumes in various parts of the system, the distribution of P_{CO_2} in the entire circuit can be calculated. For the actual calculations of these partial pressures the tubing, alveolar space, and ventilator volume are divided into segments. For each segment the P_{CO_2} is calculated repeatedly at small time intervals. These intervals are typically 10 ms, although smaller values must be used for smaller subdivisions of the tubing.

As part of this validation study, we investigated the influence of the size (volume) of the individual segments on the capnogram curves generated by the model. Table 2 gives the various subdivisions of the tubing and their respective volumes for the five models used. Inside the segments, complete and instantaneous mixing was assumed. The volumes representing the alveoli and the ventilator bellows were not subdivided. In the proximal end of the Bain circuit, where fresh gas is delivered,

Table 2. Five Subdivisions and their Volumes for the Three Tubing Sections of the Breathing System Used during Washout Experiments

	No. of Segments[a]				
Section	16	22	36	64	80
Endotracheal tube	3; 31.0	5;18.6	7;13.3	15; 6.2	17; 5.5
Bain circuit	5;102.0	7;72.9	13;39.2	23;22.2	29;17.6
Connecting tube	5;111.6	7;79.7	13;42.9	23;24.3	31;18.0

[a] The number of segments in each section and the corresponding segment volumes (in ml) are given under each column heading. The remaining three segments are the lung, the mixing segment at the proximal end of the Bain circuit, and the ventilator bellows or reservoir bag.

unpredictable mixing of fresh gas and expired gas occurs [2]. This part of the system was therefore represented as a single segment in all models. Thus, the models differed only in number of segments, which represented the endotracheal tube, the outer volume of the Bain circuit, and the connection between the Bain circuit and the ventilator (or the bag for manual and spontaneous ventilation).

The procedure for comparing the model and experimental results was to make the experimental and model gas flow patterns similar in amplitude and shape. The square-wave inspiratory flow generated by the ventilator thus created a well-defined inflow pattern while expiration was passive. Only a few parameters were left available for further adjustment of the model, including resistance of the ventilator expiratory flow control valve and of the spill valve, the values of which were not known from the specifications. Note that neither of the valves will be linear, i.e., a doubling of the flow through the valves will not cause a doubling of the pressure difference across the valves. In our earlier description of the model, we assumed a quadratic pressure–flow relation [1], but there was insufficient evidence that this was a better approximation than a linear relation. In the present study we returned to a linear pressure–flow relation for both the control and the spill valves.

The model does not incorporate the description of any inertial effects, although accelerations of the mass of gas in the tubing do occur, particularly at the onset of expiration. The effect of inertia is reduction of the initial high gas flow rate when the ventilator releases its inspiratory pressure. Resistances of the tubing and valves have a similar limiting influence on the maximum flow rate. Furthermore, inertia in the mechanical parts of the ventilator decreases the slopes of the square-wave inspiratory flow rate somewhat, whereas the model uses an exact square-wave. In the Bain model the omission of both inertia and nonlinearity is compensated for by adjusted resistances of the expiratory flow control and spill valves. Values for these resistances have been obtained from such model adjustments; the resulting values are given in Table 1.

In the second experiment, in which the test lung was ventilated manually, the objective of the anesthesiologist was to maintain an expired CO_2 level of 40 mm Hg. The exact action of the anesthesiologist's hand on the breathing bag is unknown. This action is represented in the model by an increase and a decrease in the elastance of the bag. Elastance is the ratio of pressure change and volume change, i.e., the inverse of compliance. The time course of the elastance change is discussed in the Results section. It is obvious that the anesthesiologist's action is not as exactly reproducible as mechanical ventilation is. Because model performance is identical during each cycle, there is an inherent discrepancy.

In the third experiment, in which a volunteer breathed spontaneously through a Bain circuit, the ventilatory action was represented by a negative pressure comparable to the effect of the diaphragm and intercostal muscle contraction:

$$\begin{aligned}&\text{alveolar pressure}\\&= \frac{(\text{alveolar volume} - \text{functional residual capacity})}{\text{lung thorax compliance}}\\&- \text{muscle pressure.}\end{aligned}$$

The first term on the right side of this equation represents alveolar pressure of the passive lung-thorax combination and depends only on alveolar volume. Increase in "muscle pressure" reduces alveolar pressure and causes an inspiration. Again, the time course of muscle pressure and its magnitude are unknown and must be approximated by certain functions given in the Results section.

The weight of the bag at the end of the Bain circuit causes it to collapse when open to atmospheric pressure; this was represented by a minimal elastance value. A larger elastance value represented the distensibility of the bag in a fully stretched state.

As shown later in the text, the agreement between model and experimental results is reasonable, but because models never completely represent reality there will be some discrepancies. To evaluate such differences, the influence of the accuracy of settings and of some parameter values was estimated by repeating the

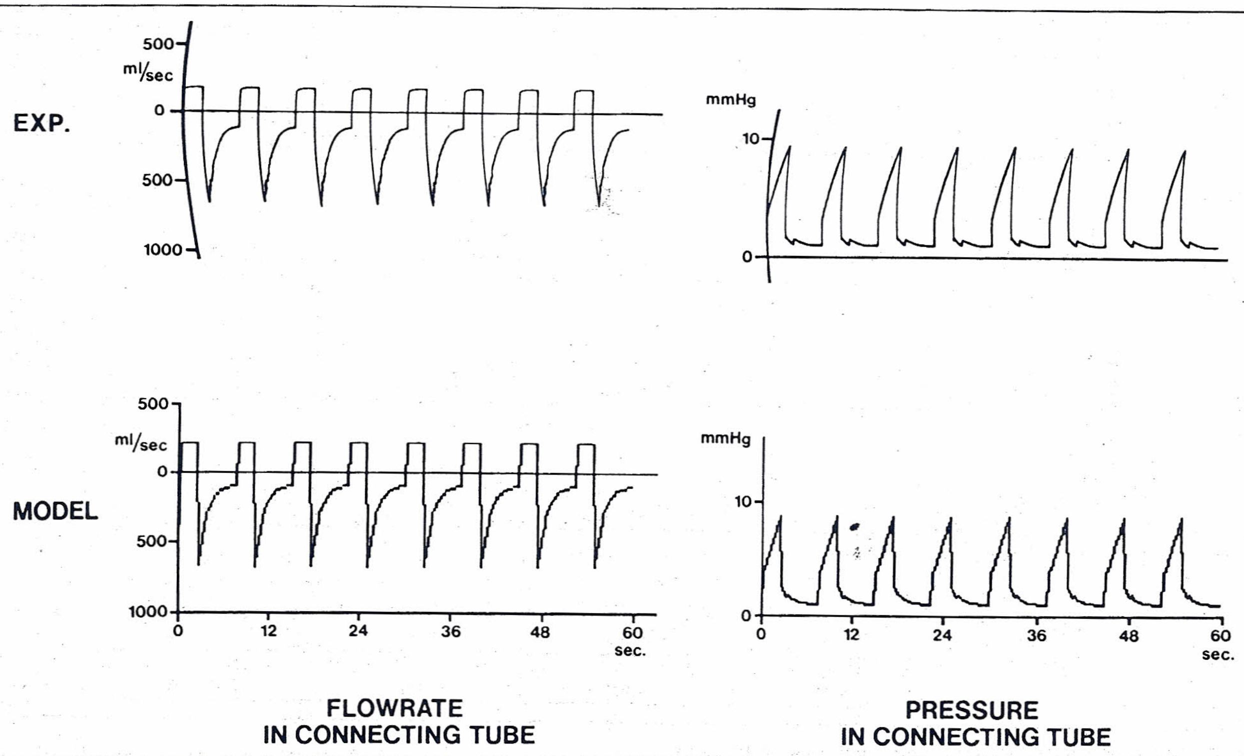

Fig 2. Experimentally obtained (upper) and model-generated (lower) time courses of pressure and flow for a fresh-gas flow rate of 5.3 L/min. The model curves show the effect of time steps in the calculation. Inspiration is upward. The end-expiratory flow does not approach zero at this point of the circuit because of the constantly flowing fresh gas.

model runs for different values and by measuring the differences in the results; this yielded a sensitivity table.

RESULTS

In the washout study all comparisons were performed at fresh-gas flow rates of 5.3 L/min and 10.3 L/min. Results of both series show comparable agreements between experimental and simulation results. Because pressures produce the driving forces and because flows are responsible for the transport of CO_2, their time courses represent important elements in the comparisons. The experimental and model curves for the standard setting of the ventilator and a fresh-gas flow rate of 5.3 L/min are shown in Figure 2.

Experimental and model-generated capnograms (fresh-gas flow rate, 5.3 L/min) from the various sampling sites are given in Figure 3. The influence of the degree of subdivision of the tubing segments on the shapes of the curves is illustrated by the slight differences between the curves obtained from the 16-, 22-, 36-, and 64-segment models, respectively.

In addition to the qualitative comparison of experiment and model by means of curve shapes, a more quantitative comparison is performed by looking at the CO_2 levels of the alveolar curves and comparing the appearance times of CO_2 at the three measuring sites (Table 3).

Levels refer to the plateaus in the CO_2 curves obtained from the test lung (see Figure 3, left column). Level ratios are equal to the ratio of a particular level and the preceding level. The first ratio equals the first level divided by the priming P_{CO_2} value; subsequent ratios (see Table 3, third column) are given as an average of the second, third, and fourth ratios. Appearance times are the differences between the time of the initial decrease in the alveolar P_{CO_2} and the time at the particular location when the P_{CO_2} reaches 10% of full scale, or 1 mm Hg in the experiment and 4 mm Hg in the model. Because of the synchronization of the two capnographs, as well as the ability to run the recorder at high speed, the experimental values can be accurately determined within 0.01 second. To see if the trend in the appearance times would continue, a model consisting of 80 segments was defined for the experiment, involving a fresh-gas flow of 10.3 L/min.

The results of the second experiment are shown on the left side of Figure 4; corresponding results from the computer model are on the right. The driving power for the inspiration of the test lung comes from the compression of the breathing bag. This was mathematically rep-

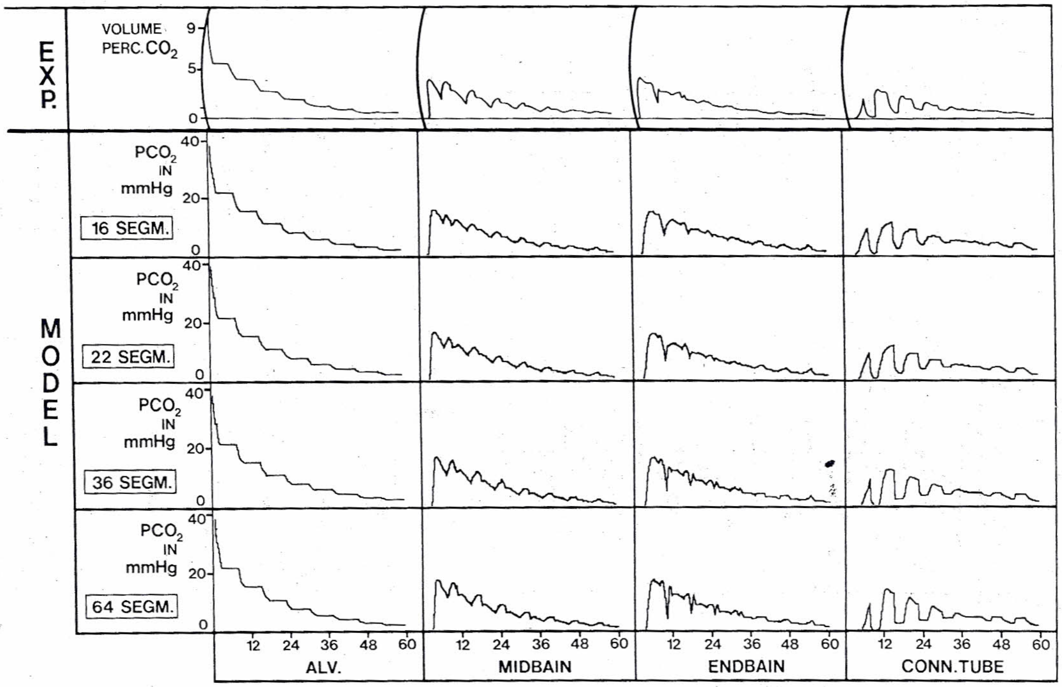

Fig 3. Comparison between experimentally obtained capnograms (top row) and model-generated capnograms (four lower rows) for the washout experiment with a fresh-gas flow rate of 5.3 L/min. The experimental curves (EXP.) *were recorded with a strip-chart recorder (Model 7D Polygraph Recorder, Grass Instruments, Quincy, MA), which caused their circular deformation. The alveolar space was primed with a gas mixture containing 9.87% carbon dioxide. The initial condition in the model was set at a partial pressure of carbon dioxide* (PCO_2) *of 40 mm Hg. Horizontal scale is time in seconds. The columns from left to right give the curves for the alveolar* (ALV.) *capnogram and the capnograms successively taken at the midpoint* (MIDBAIN) *and at the distal end of the Bain circuit* (ENDBAIN) *and close to the ventilator in the connecting* (CONN.) *tube.* PERC. = *percent;* SEGM. = *segments.*

resented by an elastance that increased according to the square root of a sine wave (part A in Figure 5). It appeared from the attempts to match the pressure and flow curves that the expiration was also controlled by the anesthesiologist and that the decrease in the elastance was gradual, as if the outflow rate were purposely limited. The decrease in elastance was represented by a cosine function raised to the third power (part B in Figure 5). The square root during inspiration created a fast rise and a relatively flat top of the curve; the third power during expiration resulted in a fast initial decline and a slow return to the expiratory value.

The describing functions for the time course of elastance variations are not unique and serve only to generate model curves for pressure and flow rate that are in agreement with the measured curves. Important to this study is the fact that once an acceptable flow rate is generated the resulting capnograms are remarkably similar.

The results of the third experiment, in which the volunteer breathed spontaneously through a Bain circuit, are shown in Figure 6, together with the corresponding model results. The driving power for the respiratory action in the model was represented by muscle pressure, as described in the Methods section. The inspiratory portion of muscle pressure has the shape of a sine wave to the power 0.8 (see part A in Figure 5); the expiratory portion is a parabolic curve to obtain a gradual transition to zero (see part B in Figure 5). The CO_2 production was estimated during model adjustment as 235 ml/min.

To explain some of the quantitative differences from the washout experiments (see Table 3), an inventory of possible sources of error was made. Three classes were distinguished: instrument, experimental, and model errors. The effect of such errors on the measurements was determined using small parameter perturbations in the computer model (Table 4). Instrument errors speak for themselves. The "unknown CO_2 wash-in" refers to the unknown quantity of CO_2 that might have washed into the test lung during the short interval between turning the three-way valve and onset of first inspiration. The effect of washing in only one-half of the "endotracheal tube" volume was determined.

The test lung shows a serious nonlinearity in the pressure–volume relation for volumes that are between 0

Table 3. Quantitative Comparison between Results of Washout and Computer Model

Fresh-Gas Flow Rate (L/min)	No. of Segments	Level Ratio		Appearance Times (s)		
		First	Subsequent	Midbain[a]	Endbain[a]	Connecting Tube
5.3	Model					
	16	0.55	0.69	3.00	3.35	5.46
	22	0.55	0.685	3.02	3.42	5.80
	36	0.55	0.68	3.06	3.53	6.33
	64	0.55	0.68	3.08	3.61	6.71
	Experiment	0.56	0.69	3.05	3.50	6.25
10.3	Model					
	16	0.50	0.58	2.89	3.13	4.16
	22	0.50	0.57	2.87	3.17	4.26
	36	0.50	0.57	2.92	3.24	4.43
	64	0.51	0.56	2.93	3.27	4.53
	80	0.51	0.56	2.93	3.29	4.58
	Experiment	0.50	0.56	2.90	3.40	4.60

[a] Midbain refers to midpoint of Bain circuit; endbain refers to endpoint of Bain circuit.

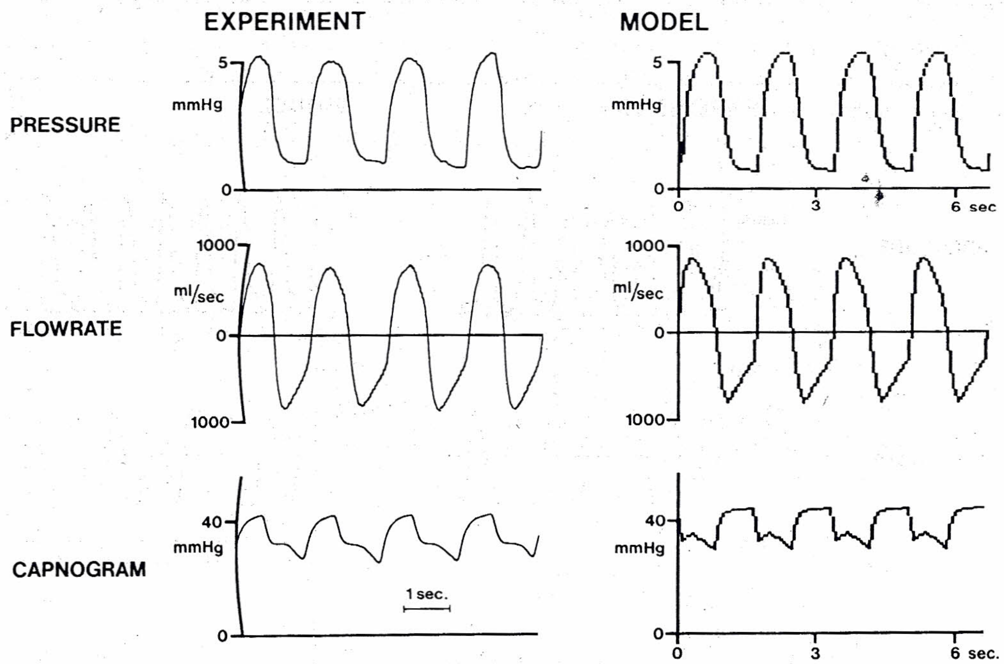

Fig 4. Comparison between experimentally obtained curves and model-generated curves for the second validation experiment, in which the test lung was ventilated manually through a Bain circuit and the fresh-gas flow was 4 L/min. The model curves were obtained at corresponding locations from a 16-segment computer model. The experimental capnogram is delayed with respect to pressure and flow curves as a result of transport delay in the sampling tube of the capnograph. The model capnogram does not exhibit this delay.

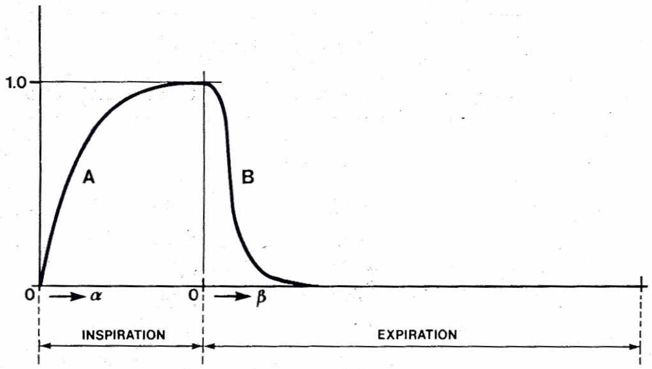

Fig 5. Model time course of inspiratory breathing bag elastance in the second and third experiments. Second experiment: curve A represents $(\sin \alpha)^{0.5}$*; curve B represents* $[(\text{cosine } \beta + 1)/2]^3$*. Third experiment: curve A represents* $(\sin \alpha)^{0.8}$*; curve B represents* β^2*.*

and 200 ml greater than minimum. In this range the compliance gradually increases from 20 ml/mm Hg to 140 ml/mm Hg for the particular setting of the compliance springs used in our experiment. The model assumes only a constant compliance value. Linearization of the experimental curve creates a negative intercept with the volume axis. This has an effect on the functional residual capacity value and CO_2 volume in the test lung, and thus on the level ratios and appearance times. Because inertial effects were not included, the sensitivity to changes in the total circuit resistance was studied. It is intuitively obvious that the maximum value of the initial expiratory flow rate has a considerable effect on appearance time. The effect of a 10% change in the resistance of the Bain circuit and the connecting tube was therefore determined. To simplify the presentation, only the sensitivity of the appearance time at the connecting tube is given.

Spoerel [3,4] took samples at seven different locations in the outer tubing of the Bain circuit. His purpose was to investigate the influence of various ventilation parameters on end-tidal and minimum inspired CO_2 concentrations. Figure 7 is a schematic representation of the maximum and minimum CO_2 concentrations Spoerel measured at these seven sampling ports [3]. Because Spoerel did not intend to perform a quantitative analysis, not all the necessary numerical data are available for an exact duplication of his experiment with our model. Instead, we used estimates of the system parameters from the washout experiment and of the patient parameters from our volunteer study. With Spoerel's ven-

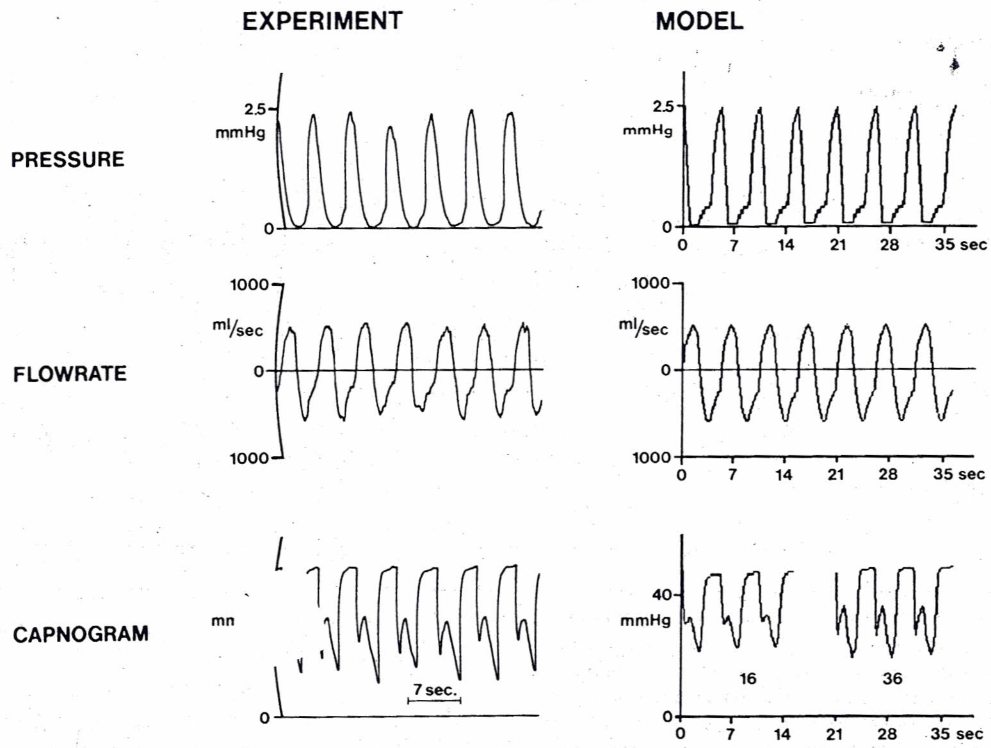

Fig 6. Comparison between experimentally obtained curves and model-generated curves for the third experiment, in which a volunteer breathed spontaneously through a Bain circuit and the fresh-gas flow was 4 L/min. Model capnograms obtained from both the 16- and the 36-segment model are shown.

Table 4. Sensitivity Data Obtained from Computer Model Measurement

Error Type	Perturbation	% Effect on Ratios		Appearance Time Changes at Connecting Tube
		First	Subsequent	
Instrument				
Fresh-gas flow setting	+3%	−0.5	−1.0	−1.0%
Minute volume setting	+10%	−5.0	0.0	−2.0%
Recorder linearity	+1%	+1.0	+1.0	0.0
Recorder zero stability	+1%	+0.5	+3.0	0.0
Experimental				
Capnogram synchronization	+0.01 s	0.0	0.0	+0.01 s
Time reading accuracy from chart	+0.03 s	0.0	0.0	+0.03 s
Unknown CO_2 wash-in	40 ml	−6.0	0.0	+0.05 s
Model				
Functional residual capacity of test lung	+10%	+3.0	+3.0	+6.0%
Circuit resistance	+10%	+1.0	+1.0	+1.5%

tilator settings, we used a special feature of the computer model, i.e., its ability to display the longitudinal distribution of CO_2 at any desired instant, or as a superposition of distributions with any desired interval (Fig 8). To avoid confusion, the superimposed longitudinal distributions for inspiration and for expiration are shown separately. Also, a computer-generated capnogram is presented to demonstrate its similarity to Spoerel's data [3].

The graphs on the left in Figure 8 are sets of superimposed distribution curves during inspiration, 300 ms apart; the lowest curve is the first and the highest is the last, immediately before expiration. In the center of Figure 8 is a similar set of graphs made during expiration. The two curves with the low CO_2 values in the endotracheal tube are the initial expiratory distributions. When the expiratory flow decreases, the diluting action of the fresh-gas flow causes a gradual decline in P_{CO_2} of the gas in the "mixing" area, which then moves slowly into the outer tubing of the Bain circuit.

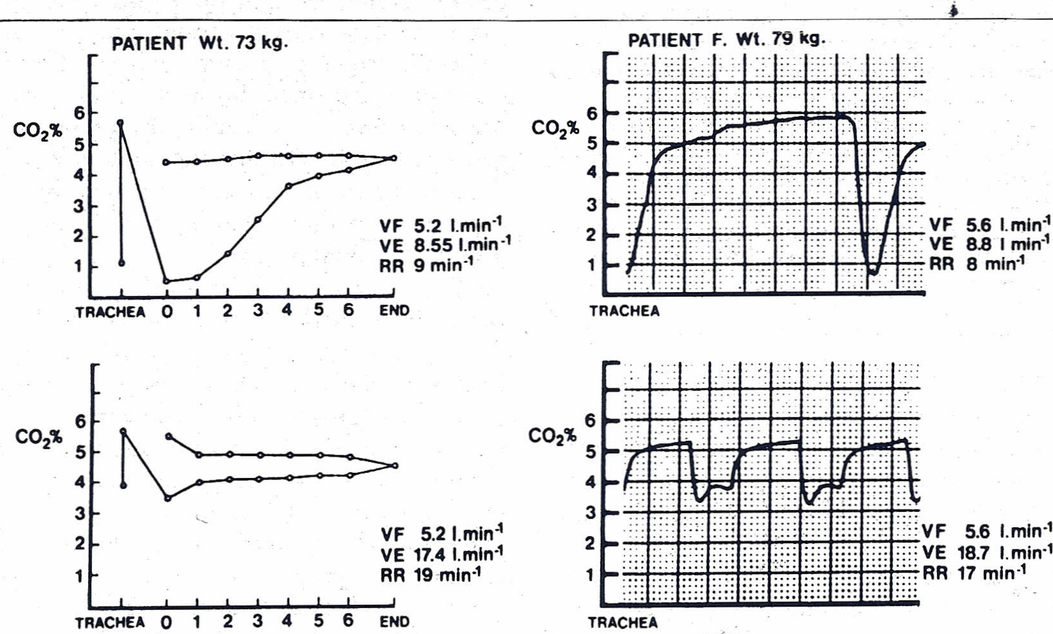

Fig 7. Measurement results of Spoerel [3]. (Left) Maximum and minimum carbon dioxide concentrations obtained in seven sampling ports distributed along the Bain circuit. Tidal volume is approximately equal in both graphs; only respiratory rate (RR) *is more than doubled in the lower graph. (Right) Two capnograms at approximately the same setting as for the results at left.* VF = *fresh-gas flow rate;* VE = *expiratory minute volume. Adapted with permission from Spoerel WE [3].*

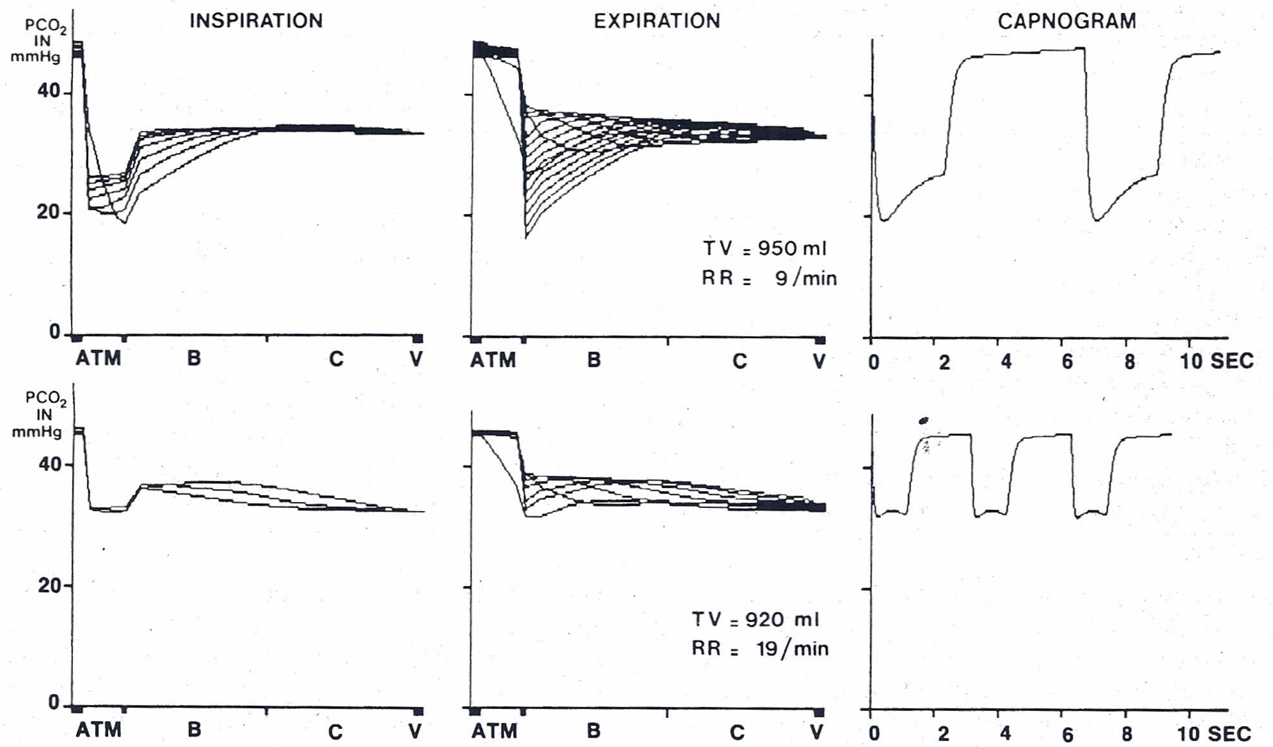

Fig 8. Longitudinal carbon dioxide distributions (the four graphs on the left) and capnograms (the two graphs on the right) obtained from the computer model, which simulates mechanical ventilation of an adult patient. For the longitudinal displays, the horizontal axis is a linear volume axis. Sections T, B, *and* C *represent, respectively, volume of the anatomical dead space and endotracheal tube (in this case, 190 ml), volume of the outer volume of the Bain circuit (510 ml), and volume of the connecting tube between ventilator and Bain arm (558 ml). Sections* A, M, *and* V *represent, respectively, the alveolar space, the mixing area where the fresh gas enters and is mixed with the inspiratory or expiratory gas, and the ventilator. These sections are not to scale; the ordinate values at these points represent the values for partial pressure of carbon dioxide* (P_{CO_2}) *in the respective volumes. Fresh-gas flow rate was set at 5.2 L/min; expiratory to inspiratory ratio was set at 2; tidal volume* (TV) *and respiratory rate* (RR) *were as indicated, to approximate the settings in Figure 7.*

DISCUSSION

The experimental setup was arranged with great care. Prevention of leaks was especially important, because leaks would cause different patterns and longer appearance times. The leak test was therefore a necessary check.

The comparison between experimental and model-generated gas flow rates and pressures (see Fig 2) clearly indicates the advantage of using a mechanical ventilator for the type of validation under study. A nearly perfect square-wave inspiratory flow can be reproduced accurately by the model. The expiration in this setup is purely passive. At the onset of expiration the ventilator opens the expiratory control valve, thus permitting the air between bellows and casing to escape. When the bellows is full, the spill valve opens and the expiratory gas is vented into the scavenging system. It is the switching from expiratory control valve to spill valve that causes the small dip in the expiratory part of the pressure curve. This detail is also present in the model-generated curve. Because the outflow is determined by the compliance of the test lung and valve resistances, an exponential outflow pattern could be expected. At the peak of the outflow curve from the experiment, some oscillations are visible, and these might possibly be caused by inertial effects in the valves. It is also likely that the gas flow around these valves becomes turbulent, particularly at high flow rates. Turbulence tends to increase the pressure difference across the valves, thus reducing the peak flow rate through the valves. Neither the inertia of the valves nor the consequence of temporary turbulence is taken into consideration in the computer model. A much more detailed study of the aerodynamic properties of these valves would be required, which is beyond the scope of this study. The consequence, however, is that the model produces slightly higher peak flow values, which we consider a major cause of the slight discrepancies found between the experiments and the model. This is the rationale behind the sensitivity test of the circuit resistance (see Table 4). A 10% change in the combined resistance to flow of the Bain circuit and the connecting tube has an effect on the peak expiratory flow rate that is similar to the effect of turbulence, thereby causing changes in the quantitative results that are large enough to explain all remaining differences.

Figure 3 is a composite figure, meant to present a fast assessment of the degree of agreement between the experiment and the computer model. A remarkable resemblance is obtained. Close inspection of the corresponding curves shows that even minor fluctuations are reproduced. There is, however, a difference between the models as a result of the number of segments. It is known from compartmental studies (e.g., in pharmacokinetics) that the mean transit time of a compartment is equal to the quotient of volume of the compartment and flow through the same compartment. Such mean transit times can also be considered as time constants (e.g., as used for describing filtering properties for certain frequencies). Table 2 shows that for each section the ratio of the volume in the 16-segment and the 64-segment model is 4.0. This means that higher frequency components are less damped in the 64-segment model than in the 16-segment model, which is reflected in the increase of peaks and valleys with an increase in the number of model segments. The curves in the top row of Figure 3 are the references. Comparing the first peak of the "ENDBAIN" (i.e., end of the Bain circuit) set of curves shows agreement between the reference and the 22-segment model. The subsequent trough of the 64-segment model is definitely too deep, and the next "shoulder" is too sharp as compared with the reference. The second peak at the connecting tube of the reference shows that the slope should be slightly negative, whereas the 16- and 22-segment models have positive slopes. The 36- and 64-segment models resemble the reference much more. The closest overall agreement with the reference, based on visual comparison, is in the 36-segment model.

A more quantitative comparison between experiment and model is presented in Table 3. The steps in alveolar P_{CO_2}, which result from successive inspirations, have been quantified as ratios of two successive levels and are in good agreement. The first step down is larger than the subsequent ones, because virtually CO_2-free gas is inspired during the first "breath"; this, in turn, is because only the "endotracheal" tube between the three-way valve and the test lung (see Fig 1) is filled with CO_2-containing gas. A source of minor uncertainty in the experiment is that the fresh-gas flow is running during the priming of the test lung. The resistance to flow of the tubing and the ventilator spill valve thus creates a pressure at the proximal part of the Bain circuit. When the three-way valve is turned, the equilibration of the pressures results in a fresh-gas displacement into the endotracheal tube. A wash-in of one-half the endotracheal tube has a 6% effect on the initial ratio and results in a 0.05-second lengthening of the appearance time at the connecting tube (see Table 3). This effect is certainly greater for higher fresh-gas flow rates and could therefore explain the slight difference in appearance times for the higher fresh-gas flow rate.

Subsequent ratios are higher than the first because some expired CO_2 mixed with other gases is reinhaled. The ratio of P_{CO_2} values in the test lung before and after dilution by an inspiration can therefore be expressed as:

$$\text{ratio} = \frac{\text{volume of test lung}}{\text{volume of test lung} + \text{VT} - \text{VD}}$$

where VT represents the inspired tidal volume and VD represents the dead space. It is interesting to mention that the subsequent ratios remain remarkably constant (see Table 3). This constancy indicates that with fixed tidal volume dead space remains constant and will consist of the known dead space of the endotracheal tube and of the "Bain circuit dead space." The latter equals the quotient of the volume of rebreathed CO_2 and the alveolar CO_2 fraction. Although the alveolar fraction (or partial pressure) decreases during subsequent breathing, the Bain circuit dead space remains constant. This suggests that extra dead space caused by rebreathing is independent of alveolar or expired CO_2 pressure. This is a confirmation of Jaeger's findings (personal communication, M. Jaeger, April 1985). It should be obvious that this extra dead space depends heavily on magnitudes of flows and flow patterns. A further investigation of these aspects is beyond the scope of the present study.

The model results relating to appearance times show an interesting phenomenon (see Table 3); a finer subdivision of the tubing yields longer appearance times. If the tubing were to be represented by only one segment, the CO_2 in the model would appear almost immediately at the end of the connecting tube (i.e., after the first 10-ms time-step of the calculation, as stated in the Model Considerations section), because the model assumes immediate and complete mixing within each of the segments. An infinite number of segments in the model would yield an appearance time determined only by tube volume and gas flow rate (mean transit time). Because flow rate is not constant, this limit cannot simply be calculated to check the model results.

Immediate and complete mixing, however, overlooks one physical phenomenon, i.e., diffusion. The flow of gas back and forth, usually in corrugated tubing, is likely to result in both axial and radial diffusion, which is difficult to quantify. The assumption of complete and immediate mixing could be considered as a way of introducing this diffusion effect into the model.

When the experimental results in Table 3 are compared with the model results, both for the two level ratios and the three appearance times, the 36-segment model scores highest, certainly for fresh-gas flow of 5.3 L/min. This is a confirmation of what was suggested in Figure 3, where on qualitative grounds the 36-segment representation was believed to be optimal. A finer subdivision in the model representation is preferred for higher gas flow rates, because of faster transport and less time for diffusion.

This discussion of optimal segment size is relevant for discovering the limitations of such model representations. Yet it should be realized that we have been discussing differences of 1 or 2% for appearance times and P_{CO_2} differences; such accuracies are hardly relevant in clinical practice. To investigate the applicability of the model under clinical circumstances, measurements during manual ventilation of the test lung with a breathing bag were recorded. Once good agreement is obtained between experimental and model gas flow rates (see Fig 4), good agreement between the capnograms will result. Agreement between the pressure tracings can be considered an additional check on the correct representation of the mechanical aspects of the model. Special attention is drawn to the extremely high respiratory rate, almost 35 breaths/min. From the calibration test we performed before the measurements, we concluded that the capnograph used for this experiment could probably not fully follow such fast changes. This explains the slightly damped appearance of the experimental capnogram as compared with the model curve.

Because of the observed interaction between "lung" properties and Bain circuit performance, the test lung in the experimental setup is useful for its reproducible and known properties and indispensable to a validation study involving lung mechanics. With the fan installed inside, the test lung performed well as a single segment with continuous and complete mixing.

The performance of the Bain circuit during spontaneous breathing can also be represented well by the model (see Fig 6). Again, once the pressures and flow rates are accurately reproduced in the model, the resulting capnogram is in agreement. To confirm the influence of segment size on the model results, the same muscle pressure driving function was used in a 16-segment and a 36-segment model. Once again the latter produced a better agreement with the volunteer's capnogram, particularly during the inspiratory phase.

From this study it is clear that an exact duplication of the flow pattern in the model is needed to obtain a good similarity between the model and the experimental capnogram. The unusual form of the describing functions for manual or spontaneous ventilation illustrates this point. We had to use sines, cosines, and parabolas to achieve these functions; even the exponents were critical (see Fig 5). A different anesthesiologist handling the bag, or a different volunteer breathing through the Bain circuit, would require different describing functions for their representation in the model. Such adjustments cannot be avoided, and they are necessary in studies that require detailed matching. This is in agreement with the results that Rose et al [5] obtained from an elegant bag-in-bottle lung model. They also described the marked influence of the respiratory waveform on the amount of fresh-gas flow required to prevent rebreathing.

When the model is applied for the purposes of demonstration, teaching, or therapeutic planning, when the ultimate determining quantity is alveolar or end-expiratory P_{CO_2}, the describing functions are not extremely critical. The model will, as a result of its reliable duplication of the real Bain circuit and its environment, estimate the amount of rebreathed CO_2 to a sufficient degree of accuracy and produce accurate predictions of alveolar or end-expiratory CO_2 pressures. This means that the model could be used to build an interactive teaching program.

Spoerel [3,4] tried with a similar setup to investigate the longitudinal distributions of CO_2 in the Bain circuit. He limited the interpretation of the results to differences in maximal and minimal concentrations. Figure 7 shows the difference in distributions that results from increasing the respiratory rate from 9 breaths/min to 19 breaths/min; a marked reduction in the CO_2 fluctuations and capnogram amplitudes can be observed. Repeating a similar experiment with the model demonstrates the same effect. (Again note that not enough data are available for an exact duplication of Spoerel's experiment, and that the flow pattern is particularly crucial for obtaining agreement between capnograms.) Model results are given in Figure 8. It is not quite clear in Spoerel's study what the "end" point concentration represents. It seems to be a dead end of the Bain arm, and intermittently sampling gas from this port probably does not yield a representative sample. We mention this because beyond the end of the Bain circuit, i.e., in the connecting tube, reasonable fluctuations still exist, as can be seen from section C in the longitudinal graphs in Figure 8. We agree with Spoerel that the availability of the longitudinal distribution gives an insight into the function of the Bain circuit. This particular feature of the developed model is therefore an important asset. The two capnograms in Figure 8 agree remarkably well with Spoerel's curves, thus supporting our statement that the function we introduced to describe a volunteer's muscle pressure is reasonably representative.

A final relationship between Spoerel's results and ours is that almost doubling the minute ventilation delivered by the ventilator produces practically no reduction in the end-expired CO_2 level (from 47.5 mm Hg to 45.8 mm Hg). This is in agreement with our sensitivity study (see Table 4) using the washout experiments. Minute volume setting has no effect on the subsequent ratios, i.e., it does not influence the earlier defined Bain circuit dead space. Rose et al [5] also showed in their experiments the reduced effectiveness of increasing the minute volume to attain a reduction in end-expired CO_2.

The Bain circuit model, as presented so far, does not contribute to important discussions relating to respiratory compensation during rebreathing [6]. This long-term adaptation is dependent on the patient's condition, the mechanism of which is not incorporated into the model.

In conclusion, this study has shown that the multisegment model can reliably explain the capnograms as well as the flow and pressure recordings when a Bain system is used. Only after a thorough validation process is it justified to promote the use of such a model for clinical management and decision making or for teaching.

REFERENCES

1. Beneken JEW, Gravenstein N, Gravenstein JS, Van Der Aa JJ, Lampotang S. Capnography and the Bain circuit I: a computer model. J Clin Monit 1985;1:103–113
2. Gravenstein N, Lampotang S, Beneken JEW. Factors influencing capnography in the Bain circuit. J Clin Monit 1985;1:6–10
3. Spoerel WE. Rebreathing and carbon dioxide elimination with the Bain circuit. Can Anaesth Soc J 1980;27:357–362
4. Spoerel WE. Rebreathing and endtidal CO_2 during spontaneous breathing with the Bain circuit. Can Anaesth Soc J 1983;30:148–154
5. Rose DK, Byrick RJ, Froese AB. Carbon dioxide elimination during spontaneous ventilation with a modified Mapleson D system: studies in a lung model. Can Anaesth Soc J 1978;25:353–365
6. Byrick RJ. Respiratory compensation during spontaneous ventilation with the Bain circuit. Can Anaesth Soc J 1980;27:96–105